Inorganic Chemistry
Article

Inorg. Chem. **2009**, *48*, 8337–8341 **8337**
DOI: 10.1021/ic900960g

Synthesis, Electronic and Crystal Structures, and Physical Studies of the Superconductor $Cs_{\sim 1}Mo_{12}S_{14}$, Final Step of the Condensation of the $Mo_6L_8^iL_6^a$ Unit

Patrick Gougeon,* Diala Salloum, Jérme Cuny, Laurent Le Pollès, Marie Le Floch, Régis Gautier, and Michel Potel

Sciences Chimiques de Rennes, UMR CNRS 6226, Université de Rennes 1, Ecole Nationale Supérieure de Chimie de Rennes, Avenue du Général Leclerc, 35042 Rennes Cedex, France

Received May 15, 2009

The ternary reduced molybdenum sulphide $Cs_{\sim 1}Mo_{12}S_{14}$ has been synthesized by solid-state reaction at 1400 °C for 96 h in sealed molybdenum crucibles. The compound crystallizes in the trigonal space group $P\bar{3}1c$ with the following lattice parameters: $a = 9.9793$ (2) Å, $c = 6.3730$ (2) Å, $Z = 1$. Its crystal structure was determined from single crystal X-ray diffraction data and consists of interconnected $Mo_6S_8^iS_6^a$ units forming an original three-dimensional framework in which large tunnels are occupied randomly by the Cs^+ ions. ^{133}Cs static NMR studies are in favor of a static cesium disorder. Unlike $Ba_4Mo_{12}S_{18}$ where some $Mo_6S_8^iS_6^a$ units are also connected through $S^{i\text{-}i}$ ligands, this connection mode does not lead to significant interactions in the title compound. Single-crystal resistivity measurements show that $Cs_{\sim 1}Mo_{12}S_{14}$ presents a metallic behavior with a superconducting transition at 7.7 K as confirmed by magnetic measurements.

Introduction

The ternary molybdenum chalcogenides $M_xMo_6X_8$ (M = Na, K, Ca, Sr, Ba, Sn, Pb, rare earth metal, 3d element; X = S, Se or Te), known as Chevrel phases, have attracted special interest because of their remarkable physical properties.[1−4] For example, $PbMo_6S_8$ is a superconductor with a critical temperature T_c as high as 15 K and high values of upper critical field H_{C2} of beyond 60 T at 4.2 K. The common structural motif in these compounds is the three-dimensional cross-linking of $Mo_6X_8X_6$ cluster units by sharing X atoms, as indicated in the formula $M_x(Mo_6X_2X_{6/2})X_{6/2}$.[5] The $Mo_6X_8X_6$ cluster unit consists of an octahedral Mo_6 cluster surrounded by 14 chalcogen atoms with eight of them forming a distorted cube and the remaining six capping the faces of the S_8 cube. In the formalism of Schäfer and von Schnering,[6] such a unit can be written as $Mo_6S_8^iS_6^a$. The ternary metal atoms, M, reside in channels running along the rhombohedral axes in this network and transfer *xn* electrons to the Mo_6 cluster as in $M_x^{n+}(Mo_6X_8^{xn-})$. Up to four electrons per Mo_6 cluster may be transferred so *xn* ranges from 0 to 4. Generally, frameworks with four transferred electrons (24 metal−metal bonding electrons per Mo_6 cluster) are semiconducting while those with $xn < 4$ are metallic and often superconducting. In 1983, we presented briefly the superconducting compound $Cs_{0.6}Mo_6S_7$[7] which presents a different arrangement of the $Mo_6S_8^iS_6^a$ units. We present here a thorough study of the latter compound which includes the synthesis, the electronic and crystal structures, and some physical studies such as magnetic, NMR, and electrical measurements.

Experimental Section

Syntheses. Starting materials used for the syntheses were MoS_2, Cs_2MoS_4 and Mo, all in powder form. Before use, Mo powder (Plansee 99.99%) was reduced under H_2 flowing gas at 1000 °C during ten hours to eliminate any trace of oxygen. The molybdenum disulfide was prepared by the reaction of sulfur (Fluka 99.999%) with H_2 reduced Mo in a ratio 2:1 in an evacuated (ca. 10^{-2} Pa Ar residual pressure) and flame-baked silica tube, heated at 800 °C during two days. The thiomolybdate of cesium was obtained by sulfuration of Cs_2MoO_4, at 450 °C, respectively, for two days using CS_2 vapor in a flowing argon carrier. The molybdate Cs_2MoO_4 was synthesized by heating an equimolar ratio of MoO_3 (CERAC 99.95%) and Cs_2CO_3 (CERAC 99.9%) in an alumina vessel at 800 °C in air over two days. The purity of all starting reagents was checked by powder X-ray diffraction on an Inel curve sensitive position detector CPS 120. Furthermore, to avoid any contamination by

*To whom correspondence should be addressed. E-mail: patrick.gougeon@univ-rennes1.fr.

(1) Fischer, Ø. *Appl. Phys.* **1978**, *16*, 1.
(2) Yvon, K. *Curr. Top. Mater. Sci.* **1979**, *3*, 53.
(3) *Superconductivity in Ternary Compounds, I*; Fischer, Ø., , Maple, M. B., Eds.; Springer: Berlin, 1982 (Top. Curr. Phys. 1982, 32).
(4) Flukiger, R. In *Superconductor Materials Science*; Foner, S., Schwartz, B., Eds.; Series B; Plenum: New York, 1981; pp 511−604.
(5) Guillevic, J.; Bars, O.; Grandjean, D. *J. Solid State Chem.* **1973**, *7*, 158.
(6) Schäfer, H.; von Schnering, H.-G. *Angew. Chem.* **1964**, *20*, 833.
(7) Gougeon, P.; Potel, M.; Padiou, J.; Sergent, M. *C. R. Acad. Sci. Paris* **1983**, *297*, 339.

Published on Web 07/31/2009

oxygen and moisture, the starting reagents were kept and handled in a purified argon-filled glovebox. Single-phase powder of $CsMo_{12}S_{14}$ was obtained by high-temperature solid state reaction from the required stoichiometric mixture of MoS_2, Cs_2MoS_4, and Mo. Theses powders were mixed, ground together in a mortar, and then cold-pressed using a hand press. The pellet was then loaded in a molybdenum crucible, which was sealed under a low argon pressure using an arc welding system. The crucible was heated at a rate of 300 °C h^{-1} to 1400 °C and held there for 4 days, then cooled at 100 °C h^{-1} to 1000 °C and finally furnace cooled to room temperature. The analysis of X-ray diagrams of powders with starting compositions ranging from $Cs_{0.9}Mo_{12}S_{14}$ to $Cs_{1.1}Mo_{12}S_{14}$ showed a single phase. Beyond these limits, multiphase samples with Mo_2S_3 and $Cs_2Mo_6S_6$ as main impurities were obtained. Crystals grow generally in the shape of an elongated hexagonal pyramid (Figure 1). The quasi-absence of nonstoichiometry in cesium was also confirmed by the X-ray studies made on single crystals coming from different preparations. Indeed, the stoichiometry in cesium was in the $Cs_{0.978(8)}Mo_{12}S_{14}$−$Cs_{1.15(1)}Mo_{12}S_{14}$ range.

Single Crystal Structure Determination. A black hexagonal bipyramidal crystal of approximate dimensions $0.110 \times 0.100 \times 0.092$ mm^3 was selected for data collection. Intensity data were collected on a Nonius Kappa CCD diffractometer using a graphite-monochromatized Mo Kα radiation ($\lambda = 0.71073$ Å) at room temperature. The frames were recorded using $\Delta\omega = 2°$ rotation scans with an X-ray exposure time of 60 s. Reflection indexing, Lorentz-polarization correction, peak integration, and background determination were performed using the program DENZO of the Kappa CCD software package.[8] An empirical absorption correction was applied with the SORTAV program[9] ($T_{min} = 0.4537$, $T_{max} = 0.5035$). Analysis of the data revealed that the systematic absence (*hhl*) $l = 2n + 1$ was consistent with the trigonal space group $P\bar{3}1c$. Of 11243 reflections collected in the 3.97−39.91° θ range, 1138 were independent ($R_{int} = 0.0288$). The initial positions for all the molybdenum and sulfur atoms were determined with the direct methods program SIR97[10] in the $P\bar{3}1c$ space group. At this stage, an electron density difference map revealed a quasi-continuous electron density along the *c* axis with a clear maximum at the levels $z = 0.25$ (Figure 2). Subsequently, different models were refined with SHELXL97[11] to describe the cesium distribution. The best one corresponded to two partly occupied Cs sites (4*e* and 2*b*) using second-order tensors for the anisotropic displacement parameters. Anharmonic treatment of atoms Cs1 and Cs2 using the program JANA2000[12] was unsuccessful. The final occupation factors for the Cs atoms were refined freely to values of 0.845(11) and 0.57(3) for Cs1 and Cs2, respectively. The positional and anisotropic displacement parameters for all atoms as well as the occupancy factors for the Cs atoms were refined to the values R1 = 0.0163, wR2 = 0.0315 for 27 parameters and 1045 reflections with $I > 2\sigma(I)$, and the residual electron densities were 0.874 and −1.081 e $Å^{-3}$. Because of the disordering of the cesium atoms, we made reciprocal-space reconstruction of different planes as well as long-exposure rotations along the *a* and *c* axes on a single crystal on the KappaCCD diffractometer. In both cases, we did not observe any superlattice reflection. A summary of the X-ray crystallographic and experimental data is presented in Table 1, and selected interatomic distances are reported in Table 2.

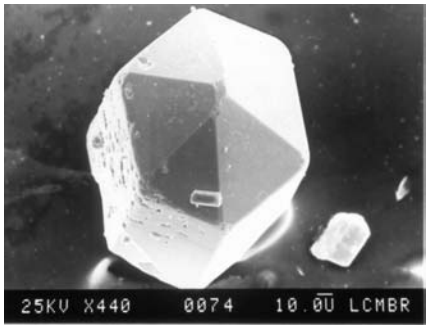

Figure 1. SEM image of a crystal of $Cs_{\sim 1}Mo_{12}S_{14}$.

Electrical Resistivity Measurements. The ac resistivity was measured on single crystals at 80 Hz with a current amplitude of 20 μA using standard four-probe techniques between 290 and 4.2 K. Ohmic contacts were made by attaching molten indium ultrasonically.

Magnetic Susceptibility Measurements. Susceptibility data were collected on a powder sample on a SHE-906 SQUID magnetosusceptometer at an applied field of 10 Oe.

Solid-State NMR Experiments. ^{133}Cs ($I = 7/2$) NMR experiments were carried out under static and MAS conditions (up to 14.5 kHz) using a Bruker Avance 300 spectrometer equipped with a 4 mm MAS probe. Rotor synchronized quadrupolar echo pulse sequences were used with radiofrequency field strength of 62 kHz and repetition delays of 2 s.

Computational Details. Self-consistent ab initio band structure calculations of $CsMo_{12}S_{14}$ were performed with the scalar relativistic tight-binding linear muffin-tin orbital method in the atomic spheres approximation including the combined correction (LMTO).[13] A model compound where cesium atoms only occupy 2*b* sites was first considered. Exchange and correlation were treated in the local density approximation using the von Barth−Hedin local exchange correlation potential.[14] Within the LMTO formalism, interatomic spaces are filled with interstitial spheres. The optimal positions and radii of these additional "Empty Spheres" (ES) were determined by the procedure described in ref 15. Ten nonsymmetry-related ES with $0.65 Å \leq r_{ES} \leq 1.57$ Å were introduced for the calculations. The full LMTO basis set consisted of 6s, 6p, and 5d functions for Cs spheres, 5s, 5p, 4d, and 4f functions for Mo spheres, 3s, 3p, and 3d functions for S spheres, and s, p, and d functions for ES. The eigenvalue problem was solved using the following minimal basis set obtained from Löwdin downfolding technique: Cs (6s), Mo (5s, 5p, 4d), S (3s, 3p), and ES (1s). The *k* space integration was performed using the tetrahedron method.[16] Charge self-consistency and the average properties were obtained from 96 irreducible *k* points. A measure of the magnitude of the bonding was obtained by computing the crystal orbital Hamiltonian populations (COHP) which are the Hamiltonian population weighted density of states (DOS).[17,18] As recommended, a reduced basis set (in which all ES LMTOs have been downfolded) was used for the COHP calculations.[19] DOS and COHP curves are shifted so that ε_F lies at 0 eV.

(8) Duisenberg, A. J. M. Ph.D. Thesis, University of Utrecht, The Netherlands, **1998**.
(9) Blessing, R. H. *Acta Crystallogr., Sect. A* **1995**, *51*, 33.
(10) Altomare, A.; Burla, M. C.; Camalli, M.; Cascarano, G. L.; Giacovazzo, C.; Guagliardi, A.; Moliterni, A. G. G.; Polidori, G.; Spagna, R. *J. Appl. Crystallogr.* **1999**, *32*, 115.
(11) Sheldrick, G. M. *SHELX97, Programs for Crystal Structure Analysis*, (Release 97-2); University of Göttingen: Göttingen, Germany, 1997.
(12) Petricek, V.; Dusek, M. *Jana2000*; Institute of Physics, Academy of Sciences of the Czech Republic: Prague, Czech Republic, 2000.
(13) (a) Andersen, O. K. *Phys. Rev. B* **1975**, *12*, 3060. (b) Andersen, O. K. *Europhys. News* **1981**, *12*, 4. (c) Andersen, O. K. In *The Electronic Structure Of Complex Systems*; Phariseau, P.; Temmerman, W. M., Eds.; Plenum Publishing Corporation: New York, 1984. (d) Andersen, O. K.; Jepsen, O. *Phys. Rev. Lett.* **1984**, *53*, 2571. (e) Andersen, O. K.; Jepsen, O.; Sob, M. In *Electronic Band Structure and Its Application*; Yussouf, M., Ed.; Springer-Verlag: Berlin, 1986. (f) Skriver, H. L. *The LMTO Method*; Springer-Verlag: Berlin, 1984.
(14) von Barth, U.; Hedin, L. *J. Phys. C* **1972**, *5*, 1629.
(15) Jepsen, O.; Andersen, O. K. *Z. Phys. B* **1995**, *97*, 35.
(16) Blöchl, P. E.; Andersen, O. K. *Phys. Rev. B* **1994**, *49*, 16223.
(17) Dronskowski, R.; Blöchl, P. E. *J. Phys. Chem.* **1993**, *97*, 8617.
(18) Boucher, F.; Rousseau, R. *Inorg. Chem.* **1998**, *37*, 2351.
(19) Jepsen, O.; Andersen, O. K. Personal communication.

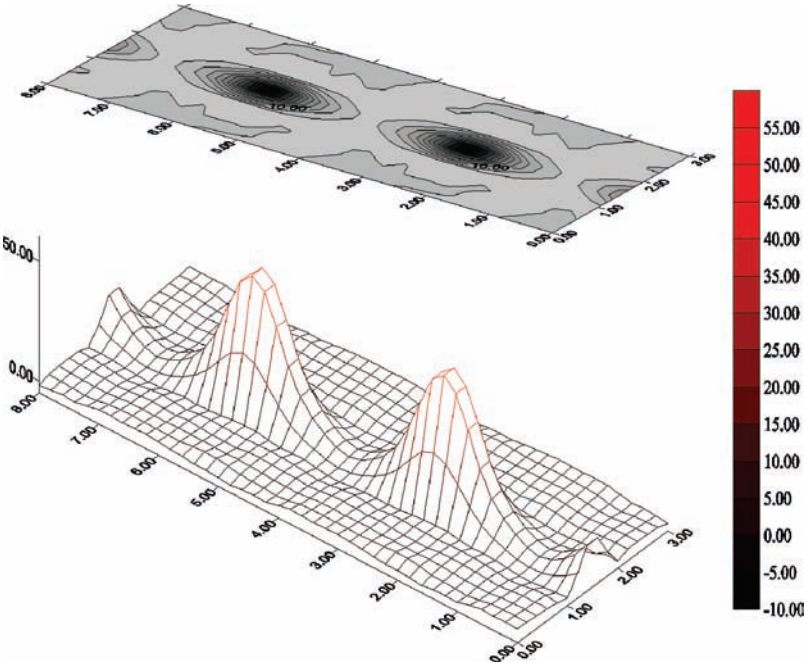

Figure 2. Difference Fourier map along the *c* axis in $Cs_{\sim 1}Mo_{12}S_{14}$.

Table 1. X-ray Crystallographic and Experimental Data for $Cs_{1.15(1)}Mo_{12}S_{14}$

formula	$Cs_{1.15(1)}Mo_{12}S_{14}$
formula weight (g mol^{-1})	1752.73
space group	$P\bar{3}1c$
a (Å)	9.9793(2)
c (Å)	6.3730(2)
V (Å^3)	549.64(2)
Z	1
ρ_{calcd} (g cm^{-3})	5.295
T (°C)	20
λ (Å)	0.71073 (Mo Kα)
μ (cm^{-1})	97.81
R1[a] (on all data)	0.0203
wR2[b] (on all data)	0.0323

[a] $R1 = \sum||F_o|-|F_c||/\sum|F_o|$. [b] $wR2 = \{\sum[w(F_o^2-F_c^2)^2]/\sum[w(F_o^2)^2]\}^{1/2}$, $w = 1/[\sigma^2(F_o^2)+(0.0279P)^2+64.3224P]$ where $P = [\max(F_o^2,0)+2F_c^2]/3$.

Full potential (linearized) augmented plane wave + local orbitals (LAPW + lo) calculations,[20] as implemented in the WIEN2K code, have also been carried out.[21] Different modeled crystallographic structures described in the space group *P*3 have been computed depending on the position of cesium atoms. Exchange and correlation effects were treated using the GGA of Perdew et al.[22] Sphere sizes of 2.5, 2.4, and 2.3 a.u. for Cs, Mo, and S spheres, respectively, were used. Basis of 57359 plane waves (corresponding to $R_{min}K_{max} = 7$) were used, and the integration was done with 36 *k* points in the irreducible Brillouin zone.

Results and Discussion

The $Cs_{\sim 1}Mo_{12}S_{14}$ compound crystallizes in an original structural type, the Mo−S three-dimensional framework of which is based on an original interconnection of the $Mo_6S^i_8S^a_6$ unit (Figure 3). The latter unit, which is similar to that encountered in the Chevrel phases, can be described as a

Table 2. Main Interatomic Distances (Å) in $Cs_{1.15(1)}Mo_{12}S_{14}$

Mo1−S1	2.4072(3)	Cs1−S1	3.5864(3) ×6
Mo1−S1	2.4341(3)	Cs1−S1	4.1287(3) ×6
Mo1−S1	2.4863(3)	Cs2−S2	3.5236(3) ×6
Mo1−S1	2.4958(3)	Cs2−S2	4.2878(3) ×6
Mo1−S2	2.61029(12)		
Mo1−Mo1	2.5999(2)		
Mo1−Mo1	2.67923(18) ×2		
Mo1−Mo1	2.7279(2)		
Mo1−Mo1$_{inter.}$	3.4962(2)		

Mo_6 octahedron surrounded by eight face-capping inner S^i (six S1 and two S2) and six apical S^a (S2) ligands. In $Cs_{\sim 1}Mo_{12}S_{14}$, all the S ligands of the $Mo_6S^i_8S^a_6$ unit are shared with the adjacent units for the first time leading to the connective formula $[Mo_6S^{i\text{-}i}_{2/2}S^{i\text{-}1}_{6/2}]S^{a\text{-}i}_{6/2}$. As a consequence the title compounds constitute the limit phase in the process of

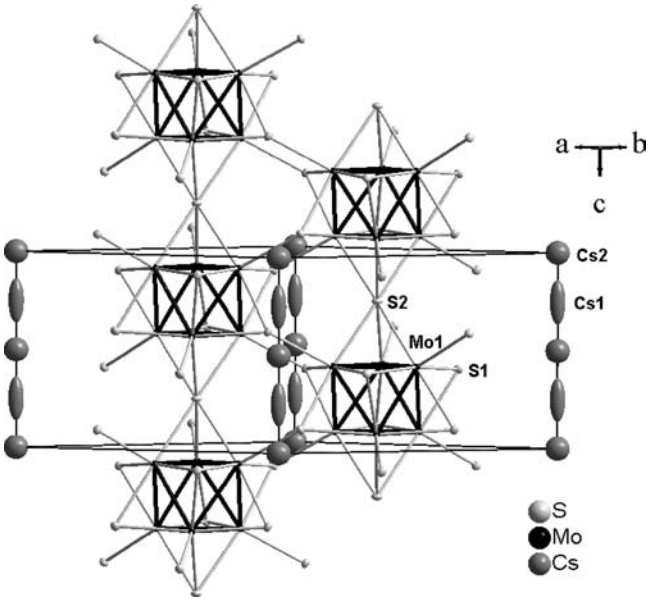

Figure 3. View of the unit-cell of $Cs_{\sim 1}Mo_{12}S_{14}$.

(20) Madsen, G. K. H; Blaha, P.; Schwarz, K.; Sjöstedt, E.; Nordström, L. *Phys. Rev. B* **2001**, *64*, 195134.
(21) Blaha, P.; Schwarz, K.; Madsen, G. K. H.; Kvasnicka, D.; Luitz, J. *Wien2k, An Augmented Plane Wave + Local Orbitals Program for Calculating Crystal Properties*; Technische Universität Wien: Wien, 2001.
(22) Perdew, J. P.; Burke, S.; Ernzerhof, M. *Phys. Rev. Lett.* **1996**, *77*, 3865.

Table 3. Progressive Condensation of the $Mo_6L^i_8L^a_6$ Unit in Reduced Molybdenum Halides, Chalcohalides, and Chalcogenides

compound	connective formula	Mo−$Mo_{intercl.}$ (Å)	VEC	transport properties	ref
$HgMo_6Cl_{14}$	$Mo_6Cl^i_8Cl^a_6$	> 6	24	insulating	23, 24
$NaMo_6Cl_{13}$	$Mo_6Cl^i_8Cl^{a\text{-}a}_{2/2}Cl^a_4$	> 6	24	insulating	25
Mo_6Cl_{12}	$Mo_6Cl^i_8Cl^{a\text{-}a}_{4/2}Cl^a_2$	4.54	24	insulating	26
$Mo_6Br_{10}S$	$Mo_6S^iBr^i_7Br^{a\text{-}a}_{6/2}$	4.50	24	insulating	27
$Mo_6Br_6S_3$	$Mo_6Br^i_4S^{i\text{-}i}_{2/2}S^{i\text{-}a}_{2/2}Br^{a\text{-}a}_{4/2}S^{a\text{-}i}_{2/2}$	3.53	24	semiconducting	29
$Mo_6S_6Br_2$	$Mo_6Br^i_2S^{i\text{-}a}_{6/2}S^{a\text{-}i}_{6/2}$	3.22	22	metallic, super., T_c = 13.8 K	1
$PbMo_6S_8$	$Mo_6S^i_2S^{i\text{-}a}_{6/2}S^{a\text{-}i}_{6/2}$	3.27	22	metallic, super., T_c = 14 K	1
$Cs_{\sim 1}Mo_{12}S_{14}$	$Mo_6S^{i\text{-}i}_{2/2}S^{i\text{-}a}_{6/2}S^{a\text{-}i}_{6/2}$	3.49	22.5	metallic, super., T_c = 7.7 K.	this work

condensation of the $Mo_6L^i_8L^a_6$ unit (L = S, Se, Te, Cl, and Br) (see Table 3). Indeed such motifs exist as discrete anions, for example, in MMo_6Cl_{14} (M = 3d divalent metal, Sn, Pb, ...)[23,24] or can be linked to each other by sharing apical and/or inner ligands to create various structure-types, the dimensionality of which depends on the numbers of shared ligands. In a first step, the sharing of the L^a ligands is observed. Thus $NaMo_6Cl_{13}$,[24,25] in which each Mo_6Cl_{14} unit shares two opposite Cl^a ligands, presents a one-dimensional character and has the connective formula $NaMo_6Cl^i_8Cl^a_4Cl^{a\text{-}a}_{2/2}$. In $MoCl_2$,[26] the Mo_6Cl_{14} units are planar linked with the formula $Mo_6Cl^i_8Cl^a_2Cl^{a\text{-}a}_{4/2}$, and in $Mo_6Br_{10}S$,[27] all the L^a ligands are shared leading to a three-dimensional arrangement the connective formula which is $Mo_6Br^i_7S^iBr^{a\text{-}a}_{6/2}$. All of the above compounds are insulators. In a second step, the inner L^i ligands are shared as exemplified by the compounds $Mo_6Br_8S_2$ ($Mo_6Br^i_5S^iS^{i\text{-}i}_{2/2}Br^{a\text{-}a}_{6/2}$),[28] $Mo_6Br_6S_3$ ($Mo_6Br^i_4S^{i\text{-}a}_{2/2}S^{i\text{-}i}_{2/2}Br^{a\text{-}a}_{4/2}S^{a\text{-}i}_{2/2}$),[29] and $M_xMo_6X_8$ (M = Na, K, Ca, Sr, Ba, Sn, Pb, rare earth metal, 3d element; X = S, Se or Te; $MMo_6S^i_2S^{i\text{-}a}_{6/2}S^{a\text{-}i}_{6/2}$), known as Chevrel phases.[1,4] The next step after the ligand sharing corresponds to the condensation of the Mo_6 cluster itself to form larger units such as Mo_9L_{11}, $Mo_{12}L_{14}$, $Mo_{15}L_{17}$, ... (L = S, Se, Te).[30] The other structural feature in $Cs_{\sim 1}Mo_{12}S_{14}$ is the connection of the $Mo_6S^i_8S^a_6$ units through $S^{i\text{-}i}$ ligands. The latter atoms are thus in a trigonal antiprismatic environment of Mo atoms. This differs from the $S^{i\text{-}i}$ ligands found in $Ba_4Mo_{12}S_{18}$,[33] in which they are in a prismatic environment of molybdenum. As reflected by the connective formula ($[Mo_6S^{i\text{-}i}_{2/2}S^{i\text{-}a}_{6/2}]S^{a\text{-}i}_{6/2}$) of the $Mo_6S_8S_6$ unit in $Cs_{\sim 1}Mo_{12}S_{14}$, they are also, similarly to the Chevrel phases, six $S^{i\text{-}a}$ and six $S^{a\text{-}i}$ ligands around each Mo_6 cluster which are shared with the six adjacent clusters, three above and three below. However, the latter ones are in the eclipsed position, while in the Chevrel phases, they are in the staggered position. It results, from this arrangement, in large channels extending along the *c* axis in which the cesium ions reside as shown by the projection of the structure onto the hexagonal plane (001) (Figure 4).

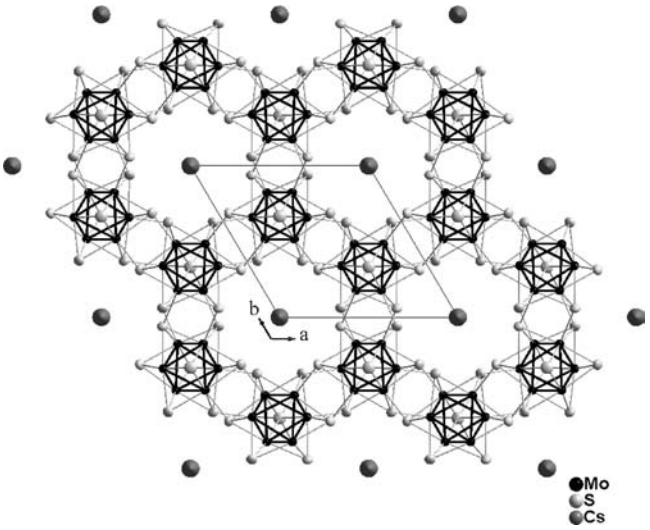

Figure 4. Crystal structure of $Cs_{\sim 1}Mo_{12}S_{14}$ as viewed down the *c*-axis. Black lines denote Mo−Mo bondings, and gray lines, Mo−S bondings. Ellipsoids are drawn at the 97% probability level.

The Mo_6 clusters are centered on 2d positions (1/3, 2/3, 1/4) and thus have here the point symmetry D_3 instead of C_{3i} in the rhombohedral $M_xMo_6X_8$ compounds. The loss of the inversion center leads to a small rotation of about 7° of the two Mo_3 triangles perpendicular to the 3-fold axis that are in the ideal staggered conformation in the rhombohedral $M_xMo_6X_8$ compounds. As a consequence, two different intertriangle Mo−Mo distances of 2.5999(2) and 2.7279(2) Å are observed in $CsMo_{12}S_{14}$. The Mo−Mo intratriangle distances which correspond to the distances within the Mo_3 triangles formed by the Mo atoms related through the 3-fold axis are equal to 2.67923 (18) Å in $CsMo_{12}S_{14}$. The averaged Mo−Mo distance is 2.672 Å. The Mo atoms are surrounded by five S atoms (4 S1 and 1 S2) forming a distorted square pyramid. The Mo−S1 bond distances range from 2.4072(3) to 2.4958(3) Å while the Mo−S2 distance is longer and equal to 2.61029(12) Å. This also leads to an intercluster distance of 3.4962(2) Å. It is interesting to note that the latter distance is larger that those observed in the sulfides $M_xMo_6S_8$ where they do not exceed 3.4086(3) Å as observed in $BaMo_6S_8$.[31] The sulfur cavities occupied by the cesium atoms can be described as highly distorted snub tetrahedra with Cs−S distances ranging from 3.5236(3) to 4.2878(3) Å.

Electrical resistivity measurements were performed on a single crystal of composition $Cs_{0.978(8)}Mo_{12}S_{14}$ that was determined from an X-ray study. $CsMo_{12}S_{14}$ is poorly metallic, with a room temperature resistivity of 1.4 mΩ·cm,

(23) von Schnering, H.-G. *Z. Anorg. Allg. Chem.* **1971**, *385*, 75.
(24) Potel, M; Perrin, C; Perrin, A.; Sergent, M. *Mater. Res. Bull.* **1986**, *21*, 1239.
(25) Boeschen, S.; Keller, H. L. *Z. Kristallogr.* **1991**, *196*, 159.
(26) Schäfer, H.; von Schnering, H. G.; Tillack, J. V.; Kuhnen, F.; Woehrle, H.; Baumann, H. *Z. Anorg. Allg. Chem.* **1967**, *353*, 281–310.
(27) Perrin, C.; Sergent, M.; Le Traon, F.; Le Traon, A. *J. Solid State Chem.* **1978**, *25*, 197.
(28) Perrin, C.; Sergent, M *J. Chem. Res.* **1983**, *2*, 38.
(29) Perrin, C.; Potel, M.; Sergent, M. *Acta Crystallogr., Sect. C: Cryst. Struct. Commun.* **1983**, *39*, 415.
(30) (a) Gougeon, P.; Potel, M.; Padiou, J.; Sergent, M. *Mater. Res. Bull.* **1987**, *22*, 1087–1093. (b) Gougeon, P.; Potel, M.; Padiou, J.; Sergent, M. *Mater. Res. Bull.* **1988**, *23*, 453–460. (c) Thomas, C.; Picard, S.; Gautier, R.; Gougeon, P.; Potel, M. *J. Alloys Compd.* **1997**, *262 - 263*, 305–310. (d) Picard, S.; Gougeon, P.; Potel, M. *Angew. Chem., Int. Ed.* **1999**, *38*, 2034–2036.
(31) Kubel, F.; Yvon, K. *Acta Crystallogr., Sect. C: Cryst. Struct. Commun.* **1990**, *46*, 181.

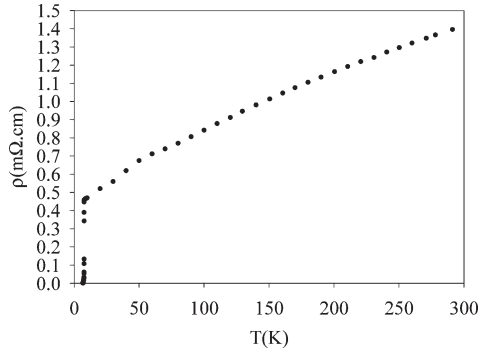

Figure 5. Temperature dependence of the electrical resistivity for $Cs_{\sim 1}Mo_{12}S_{14}$.

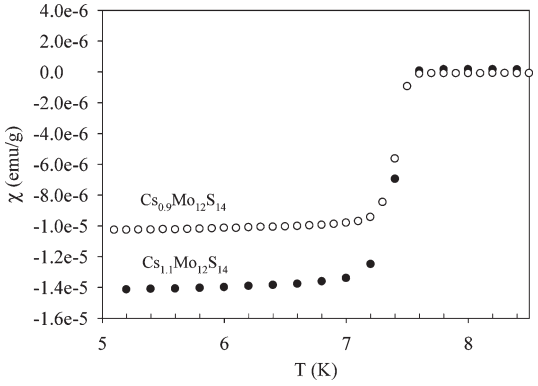

Figure 6. Temperature dependence of the dc susceptibility of $Cs_{\sim 1}Mo_{12}S_{14}$ at low temperature under an applied field of 10 Oe.

and becomes a superconductor below 7.7 K (Figure 5). The resistivity just before the superconducting transition was 0.45 mΩ·cm. Superconductivity was also confirmed by Meissner effect from susceptibility measurements on powder samples of compositions $Cs_{0.9}Mo_{12}S_{14}$ and $Cs_{1.1}Mo_{12}S_{14}$ (Figure 6). It is interesting to note the superconducting transition temperature does not change with the Cs content.

Because of the staggered conformation of the Mo_6 clusters in the title compound, the shortest Mo−Mo distance between neighboring Mo_6 clusters that share a capping sulfur ligand is equal to 4.439 Å. Such a long distance prevents the occurrence of metal−metal bonds between these clusters. That differs from the $(Mo_6)_2$ dimeric units of $Ba_4Mo_{12}S_{18}$ where a metal−metal bond links the Mo_6 octahedral units in eclipsed conformation.[33] Therefore, as for the Chevrel phases,[32] the band structure of the title compound derives from the electronic structure of the Mo_6L_8 octahedral motif, and as shown by the COHP curves sketched in Figure 7, a band gap separates the Mo−Mo bonding and nonbonding bands (MOs) from the Mo−Mo antibonding bands for the metallic electron (ME) count of 24 per Mo_6 cluster. Since the ME count per Mo_6 in the title compound is equal to 22.5, the Fermi level cuts a weakly Mo−Mo bonding peak of density of states of the valence band. That is consistent with the measured metallic properties. As for the Chevrel phases,[32] weak interactions between metal atoms of Mo_6 clusters that

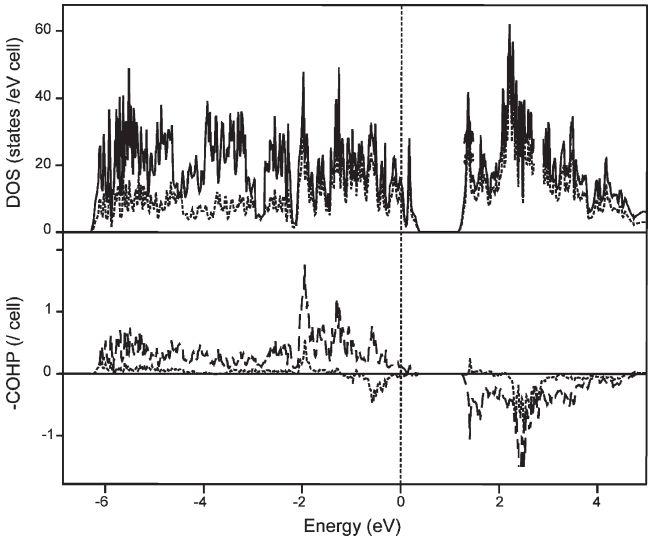

Figure 7. DFT calculations for $CsMo_{12}S_{14}$ (upper) total (solid) and Mo projected (dotted) and DOS (lower) averaged COHP for Mo−Mo bonds of the Mo_6 unit (solid) and between Mo_6 clusters that share $S^{i\text{-}a}$ and $S^{a\text{-}i}$ ligands (dotted).

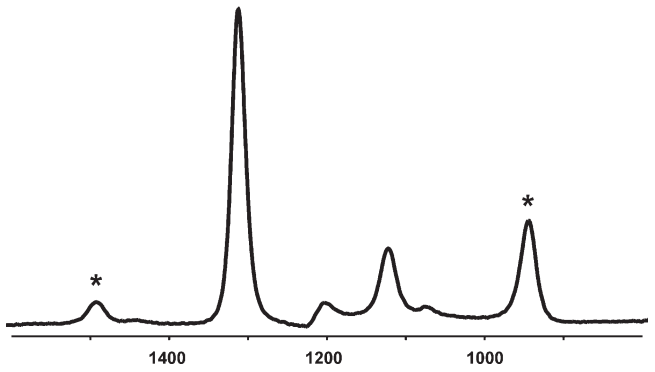

Figure 8. ^{133}Cs MAS NMR spectrum at MAS rate of 14.5 kHz. Spinning sidebands are indicated by asterisks.

share $S^{i\text{-}a}$ and $S^{a\text{-}i}$ ligands (Mo−Mo = 3.4962(2) Å) are at the origin of the metallic properties.

The ^{133}Cs static NMR spectra sketched in Figure 8 exhibit a complex line shape with overlapping signals, hindering a precise analysis of this spectrum; however, we do observe satellite transitions. This supports the hypothesis of a static cesium disorder. In the case of dynamic disorder, low frequency dynamics would average out the ^{133}Cs satellite transitions by motional narrowing.[34] Total energy calculations with DFT formalism have been performed for different crystal structures that slightly differ from the position of cesium atoms. This latter has been moved gradually from the (0, 0, 1/4) position to the (0, 0, 1/2) site. The computed total energy per unit cell increases approximately 0.025 eV when the alkaline metal occupies the latter position. Such an energy difference is consistent with the X-ray electron density map that reveals a quasi-continuous electron density along the *c* axis with maximum values for the (0, 0, 1/4) site.

Supporting Information Available: X-ray crystallographic file for $Cs_{1.15}Mo_{12}S_{14}$, in CIF format. This material is available free of charge via the Internet at http://pubs.acs.org.

(32) Hughbanks, T. *Prog. Solid State Chem.* **1989**, *89*, 329.
(33) Salloum, D.; Gautier, R.; Potel, M.; Gougeon, P. *Angew. Chem., Int. Ed.* **2005**, *44*, 1363.
(34) Ashbrook, S. E.; Whittle, K. R.; Le Pollès, L.; Farnan, I. *J. Am. Ceram. Soc.* **2005**, *88*(6), 1575.